ChemistrySelect

Research Article
doi.org/10.1002/slct.202304190

Chemistry Europe
European Chemical Societies Publishing

www.chemistryselect.org

Synthesis of 1-phenyl-3-(quinolin-8-ylamino)prop-2-en-1-one and analysis of its structure by X-ray crystallography, NMR, UV-Vis spectroscopy and DFT calculations

Michael Yu. Volkov,*[a] Alsu R. Sharipova,[a] Olga A. Turanova,[a] Aidar T. Gubaidullin,[b] Amina F. Shaidullina,[c] Ludmila I. Savostina,[a, c] and Alexander N. Turanov[a]

1-phenyl-3-(quinolin-8-ylamino)prop-2-en-1-one was obtained by a two-step synthesis. From X-ray crystallography, NMR and UV-vis spectra it follows that in the crystalline state and in solutions, regardless of the polarity of the solvent, 1-phenyl-3-(quinolin-8-ylamino)prop-2-en-1-one exists in the ketone form of the cis-isomer. DFT calculations confirmed that the cis-isomer is the most energetically favorable among all its isomers.

Introduction

β-Enaminones are universal reagents in a wide variety of syntheses because their characteristic pentad of atoms allows them to readily react with both electrophiles and nucleophiles.[1–3] Their high reactivity makes them convenient and often indispensable building blocks for the synthesis of N-heterocycles.[5] β-enaminones are of particular interest as biologically active substances. These compounds are widely used in the creation of antibacterial, antidiabetic, anti-inflammatory, anticonvulsant and antitumor agents.[5,6] β-enaminone molecules having a chelate structure are wide used as ligand systems.[7–11] The presence of double bonds in β-enaminone molecules determines the possibility of their cis-trans isomerization. The study of isomerization processes of β-enaminones is important for both applied and fundamental science[12,6] and NMR, UV spectroscopy and some other methods are suitable for this.[13–15]

In this work the synthesis, structure and identification of isomers of 1-phenyl-3-(quinolin-8-ylamino)prop-2-en-1-one is considered.

Due to limited rotation around the C=C double bond, β-enaminone molecules can exist in the form of cis- and trans-isomers (see Figure 1). Formation the cis-isomer (stabilized by an intramolecular hydrogen bond) most easily occurs in non-polar mediums, since they provide conditions for the preservation of the intramolecular hydrogen bond. At the same time, in polar solvents the probability of the existence of the trans-isomer increases due to the possible formation of intermolecular hydrogen bonds. Bulky substituents usually additionally stabilize the trans-isomer.[16,17]

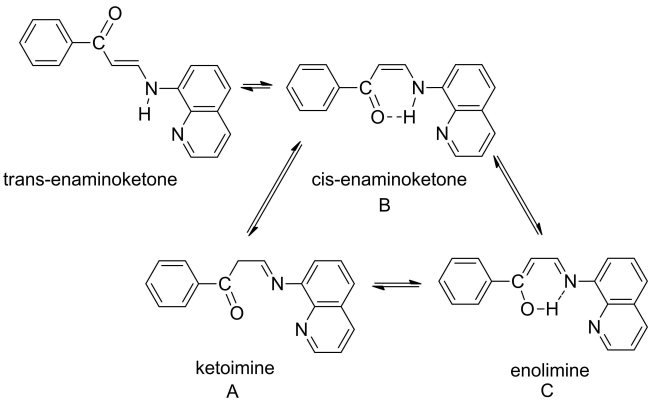

Figure 1. Isomers of 1-phenyl-3-(quinolin-8-ylamino)prop-2-en-1-one.

The ketoimine form (A) can exist in sterically strained systems. The transition to the enolimine form (C) occurs, as a rule, if there is a significant gain in the conjugation energy of the molecule as a whole (for example, the formation of a pseudo-aromatic ring). This form can be stabilized by some structural fragments, such as, for example, aromatic rings.[18] The enaminoketone form (B) is the most stable due to the presence of a strong hydrogen bond and the formation of a pseudo-aromatic ring, which increases the thermodynamic stability of the molecule.[19] A large amount of evidence has been collected using NMR, UV, IR spectroscopy as well as X-ray crystallography which showed that the most of the β-enaminones exists in the tautomeric enaminoketone form.[19–21]

The structure of the molecule, the electronic contribution and volume of substituents, intramolecular hydrogen bonds,

[a] Dr. M. Y. Volkov, A. R. Sharipova, Dr. O. A. Turanova, Dr. L. I. Savostina, Dr. A. N. Turanov
Zavoisky Physical-Technical Institute
FRC Kazan Scientific Center of RAS
Kazan, Sibirsky tract, 10/7, 420029, Russia
E-mail: mihael-volkov@yandex.ru

[b] Dr. A. T. Gubaidullin
Arbuzov Institute of Organic and Physical Chemistry
FRC Kazan Scientific Center of RAS
Kazan, Arbuzov str. 8, 420088, Russia

[c] A. F. Shaidullina, Dr. L. I. Savostina
Institute of Physics
Kazan Volga Region Federal University
Kazan, Kremlyovskaya str. 18, 420008, Russia

Supporting information for this article is available on the WWW under https://doi.org/10.1002/slct.202304190

temperature and solvent polarity affects both the tautomerization process and the isomerization process.[22]

Tautomerization processes lead to a rearrangement of electronic levels, which to some extent affects other properties of molecular systems. Thus, for example, tautomeric chains embedded in a polymer can act as a switch regulating the electronic properties of the conjugated system through the polymer backbone, thereby creating the ability to control the optical parameters of the polymer.[23]

Experimental Section

Materials

All reagents were purchased from commercial sources and used without further purification. All the used solvents were preliminarily purified by distillation until their constants coincided with the literature data. Deuterated acetone was used without prior purification. Elemental analysis was performed on an EuroVector EA3000 CHNS–O Elemental Analyzer. Melting points were measured using optical microscope Boetius equipped with a heating stage.

Recording of NMR spectra

All ^{1}H and ^{13}C NMR spectra of the solutions were recorded by a Bruker Avance 400 NMR spectrometer at room temperature. 1-phenyl-3-(quinolin-8-ylamino)prop-2-en-1-one was dissolved at a concentration of 50 mmol/L in the following solvents: carbon tetrachloride, deuterated acetone and deuterated dimethyl sulfoxide. The resulting solutions were placed in a 5 mm glass tubes. The carrier frequencies for the ^{1}H and ^{13}C nuclei were 400 and 100 MHz, respectively. During the record of ^{1}H NMR spectra the following acquisition parameters were used: the duration of 90° pulse – 10 μs, the spectrum width – 7 kHz, delay between scans – 15 s and number of scans – 128. During the record of ^{13}C NMR spectra with proton decoupling the following acquisition parameters were used: the duration of 90° pulse – 10 μs, the spectrum width – 25 kHz, delay between scans – 15 s and number of scans – 4096. During the record of ^{13}C NMR spectra without proton decoupling the following acquisition parameters were used: the duration of 90° pulse – 10 μs, the spectrum width – 21 kHz, delay between scans – 5 s and number of scans – 65536. The ^{1}H and the ^{13}C NMR spectra of the substance in deuterated acetone and deuterated dimethyl sulfoxide were calibrated by the signal of the residual protons and the signal of the methyl groups of the solvent, respectively.[24] The ^{1}H NMR spectrum of the substance in carbon tetrachloride was calibrated by the signal of chloroform,[25] which was added into the solution at a concentration of 1 mmol/L. The ^{13}C NMR spectrum of the substance in carbon tetrachloride was calibrated by the signal of the solvent.[26] In the Fourier transform of the obtained FIDs, a 1-Hz line broadening for ^{1}H spectra and 3-Hz line broadening for ^{13}C spectra were applied.

During the record of ^{1}H–^{1}H gradient-selected multiple-quantum filtered 2D COSY NMR spectra (Bruker pulse program "cosygpmfqf")[27,28] the following acquisition parameters were used: ^{1}H spectrum width – 7.2 kHz, delay between scans – 6 s, number of scans – 8, the duration of the gradient pulses – 2 ms, number of points in the FID – 4096 and number of t_1 increments – 1024. The spectra were zero-filled to a final size of 4096×4096 prior to Fourier transformation. During the record of ^{1}H–^{1}H 2D NOESY NMR spectra (Bruker pulse program "noesyph")[29] the used parameters were: ^{1}H spectrum width – 3.2 kHz, delay between scans – 11 s, number of scans – 16, number of points in the FID – 4096 and number of t_1 increments – 256. The spectra were zero-filled to a final size of 4096×4096 prior to Fourier transformation. The mixing time was 1.2 s for the CCl_4 solution, 2.2 s for the acetone-D_6 solution and 0.8 s for DMSO-D_6 solution. These values were chosen on the base of the relaxation times T_1 determined by the inversion-recovery pulse sequence for some NMR signals of interest in these solutions.

During the record of ^{1}H–^{13}C phase sensitive gradient-enhanced 2D HSQC NMR spectra with using echo-antiecho coherence selection (Bruker pulse program "hsqcetgpsi2")[30,31] the following acquisition parameters were used: ^{13}C spectrum width – 6.2 kHz, ^{1}H spectrum width – 3.6 kHz, delay between scans – 6 s, number of scans – 16, the duration of the gradient pulses – 1 ms, number of points in the FID – 2048 and number of t_1 increments – 512. The spectra were zero-filled to a final size of 2048×2048 prior to Fourier transformation. During the record of ^{1}H–^{13}C gradient-enhanced 2D HMBC NMR spectra with using low-pass J-filter (Bruker pulse program "hmbcgplpndqf")[32] the following acquisition parameters were used: ^{13}C spectrum width – 11.3 kHz, ^{1}H spectrum width – 3.7 kHz, delay between scans – 5 s, number of scans – 16, the duration of the gradient pulses – 1 ms, number of points in the FID – 4096 and number of t_1 increments – 512. The spectra were zero-filled to a final size of 4096×4096 prior to Fourier transformation.

The evolution time in 2D HSQC NMR experiments was optimized for a one-bond C–H scalar coupling of 164 Hz. For each of the solutions, three separate 2D HMBC NMR spectra were recorded with evolution times optimized for multiple C–H bond couplings of 7.0, 3.7 and 1.2 Hz, respectively. Then these three 2D HMBC NMR spectra of each of the solutions were combined into one total spectrum. All the above-mentioned C–H coupling constants were found on the base of the ^{13}C NMR spectra of the studied substance recorded without proton decoupling. The data acquisition and also the processing of 1D and 2D NMR spectra were carried out by the Bruker XWIN-NMR 3.5 software.

Recording of electronic and emission spectra

The electronic spectra of the substance were recorded in various organic solvents of different polarity (hexane, carbon tetrachloride, chloroform, acetone, acetonitrile, dimethyl sulfoxide) at a concentration of 4.4×10^{-5} mol/L. The electronic spectra were recorded on a Varian Cary 100 spectrophotometer using 10 mm quartz cell at room temperature in the range from 200 to 800 nm at a speed 600 nm/min and a slit width of 1.5 nm. The spectra of fluorescence were studied with a Fluorat-02-Panorama spectrofluorimeter (Lumex, Russia). The emission spectra of compound were recorded between 400 and 600 nm, every 1 nm, with excitation wavelength set at 440 nm. Excitation at longer wavelengths was not used because it results in emission with lower intensity. UV irradiation of the solutions used both for recording the electronic absorption spectra and for recording the NMR spectra was carried out by a Vilber Lourmat lamp with a power of 6 W in the irradiation mode indicated by the manufacturer as 365 nm.

Collecting of X-ray diffraction data

The X-ray diffraction data for the crystal of 1-phenyl-3-(quinolin-8-ylamino)prop-2-en-1-one were collected by a Bruker D8 Quest single crystal X-ray diffractometer equipped with an Incoatec IμS microfocus source (Mo Kα, λ = 0.71073 Å), a multilayers optics monochromator and a PHOTON III area detector, in the ω and φ-scan modes at 100(2) K. The frames were integrated with the Bruker SAINT software package using a narrow-frame algorithm. Data were

corrected for absorption effects using the Multi-scan method by SADABS program.[33] The structure was solved by direct method using SHELXS and refined by the full matrix least-squares using SHELXTL programs.[34] All non-hydrogen atoms were refined anisotropically. The hydrogen atoms were inserted at calculated positions and refined as riding atoms except the hydrogen atom of amino-group, which was determined on the base of the electronic density distribution and was refined isotropically. Data collection: images were indexed and integrated using the APEX3 data reduction package.[35] All calculations were performed on PC using WinGX suit of programs.[36] Analysis of the intermolecular interactions was performed using the program PLATON.[37] The Mercury program package[38] was used for the figures preparation.

Carrying out of quantum chemical calculations

Quantum-chemical calculations of the molecular structure, energies of states of the isomers, as well as UV spectra were performed by the ORCA software package.[39] The DFT method using the CAM–B3LYP functional[40] and the def2-TZVP basis set[41] were applied. Solvent molecules were not taken into account in the calculations.

Synthesis scheme of β-oxymethyleneacetophenone and 1-phenyl-3-(quinolin-8-ylamino)prop-2-en-1-one

Sodium salt of β-oxymethyleneacetophenone: metallic sodium (2.17 g, 0.094 mol) and benzene (20 ml) were added to the mixture of ethyl formate (7.6 ml, 0.094 mol) and acetophenone (11.02 ml, 0.094 mol) cooled to 5 °C. The reaction mixture was stirred for 20 hours, while its temperature gradually increased to room temperature. The resulting yellow precipitate was filtered off and then washed with benzene and ether. Then it was air-dried. Yield 51 %. $T_M > 300$ °C. Found, %: C 63.53; H 4.15. $C_9H_7NaO_2$. Calculated, %: C 63.62; H 4.37.

1-phenyl-3-(quinolin-8-ylamino)prop-2-en-1-one: a mixture of aminoquinoline (0.49 g, 0.003 mol) and hydrochloric acid (0.3 ml, 0.003 mol) in ethanol was added to a solution of sodium salt of β-oxymethyleneacetophenone (0.57 g, 0.003 mol) in the same solvent. The reaction mixture was boiled for 2 hours and then part of the solvent was distilled off and left at room temperature until the next day. The precipitate was filtered off and washed out with hot chloroform. The filtrate was evaporated and ethanol was added. The resulting yellow crystals were filtered off and recrystallized twice from ethanol. Yield 40 % (after two recrystallizations). $T_M =$ 129 °C. UV-Vis spectrum (CH_3CN, λ, nm (ε, $dm^3\ cm^{-1}\ mol^{-1}$): 391 (28016), 325 (3409). Found, %: C 78.89; H 5.11; N 10.20. $C_{18}H_{14}N_2O$. Calculated, %: C 78.81; H 5.14; N 10.21.

Results and Discussion

Stages of 1-phenyl-3-(quinolin-8-ylamino)prop-2-en-1-one synthesis

β-Enaminone is obtained from acetophenone by a two-step synthesis (see Figures 2 and 3). It is assumed that in the beginning sodium reacts with traces of ethanol present in the initial ethyl formate and forms catalytic amounts of sodium ethylate. The carbanion generated by the action of sodium ethylate from acetophenone is added to the carbon atom of the carbonyl group of ethyl formate. The resulting anionic

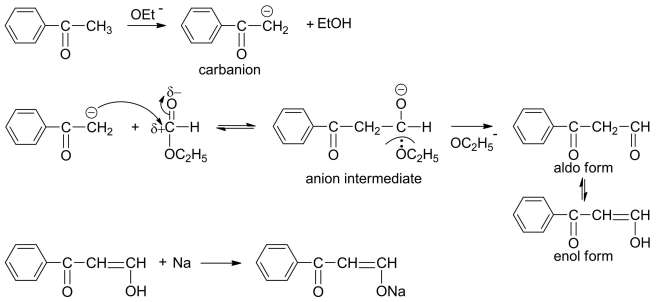

Figure 2. Possible mechanism of the first stage of enaminone synthesis.

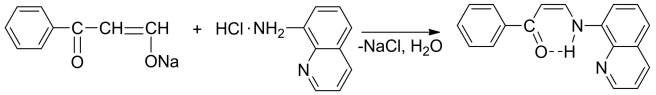

Figure 3. Second stage of the synthesis of the enaminone.

intermediate detaches the ethoxyanion and becomes stabilized in the form of β-ketoaldehyde. The increased acidity of the hydrogen atoms of the CH_2 group causes enolization of the aldehyde group. Subsequent interaction of the enol form with sodium leads to the formation of the sodium salt of β-oxymethyleneacetophenone.

Mixing the reagents leads to strong heating of the reaction mixture, therefore the reaction is carried out under slight cooling with the addition of cold benzene. The product is a high-melting yellow powder.

1-phenyl-3-(quinolin-8-ylamino)prop-2-en-1-one is obtained by boiling aminoquinoline hydrochloride and the sodium salt of β-oxymethyleneacetophenone in ethanol. The yellow crystalline precipitate was filtered off and air-dried.

The chemical structure of all obtained compounds was fully characterized by UV-Vis, ^1H and ^{13}C NMR spectroscopy and elemental analysis. The final product is also characterized by X-ray crystallography. Single crystals were obtained by second recrystallization of the product from ethanol. Crystals formed within 24 hours.

Molecular structure from X-ray crystallography

The crystal data and the refinement parameters are given in Table 1. According to the obtained data, 1-phenyl-3-(quinolin-8-ylamino)prop-2-en-1-one crystallizes from ethanol individually as a cis-isomer in the enaminoketone form (**B**) (see Figure 1). The geometry of the molecule of the substance is close to flat, however, there is some turn of the aminoquinoline and phenyl rings relative to the plane of the central pseudo-aromatic ring formed due to a strong intramolecular hydrogen bond N11–H11…O14 (d(N11–H11) 0.91(3) Å, d(H11…O14) 2.02(2) Å, d(N11…O14) 2.675(2) Å, ∠(N11–H11…O14) 128(2)°) (see Figure 4). The corresponding angles are 18.07(8)° and 11.84(7)°, while the angle between the planes of the aminoquinoline and phenyl rings is 10.78(9)°. The aminoquinoline bicycle is slightly deviated from the flat shape and its six-membered rings make

Table 1. Experimental crystallographic data for 1-phenyl-3-(quinolin-8-ylamino)prop-2-en-1-one.

Formula	$C_{18}H_{14}N_2O$
Crystal class	Orthorhombic
Space group	*Pna2*$_1$
Z, Z'	4, 1
Cell parameters	*a* = 19.7848(11) Å, *b* = 12.7239(7) Å, c = 5.4267(3) Å
V, Å^3	1366.12(13) Å^3
M (g/mol)	274.31
T, K	100(2)
Size, mm	0.052×0.081×0.428
F(000)	576
ρ_{calc} g/cm^3	1.334
μ, cm^{-1}	0.84
θ, deg	$2.608 \leq \theta \leq 28.951$
Refl. Meas.	25687
Independ/Rint	3402/0.1030
Completeness	99.6%
Param./restr	194/1
Refl. [$I > 2\sigma(I)$]	2676
R_1/wR_2	0.0483/0.1021
R_1/wR_2 (all refl.)	0.0661/0.1070
Goodness-of-fit	0.995
ρ_{max}/ρ_{min} (eÅ^{-3})	0.205/-0.218

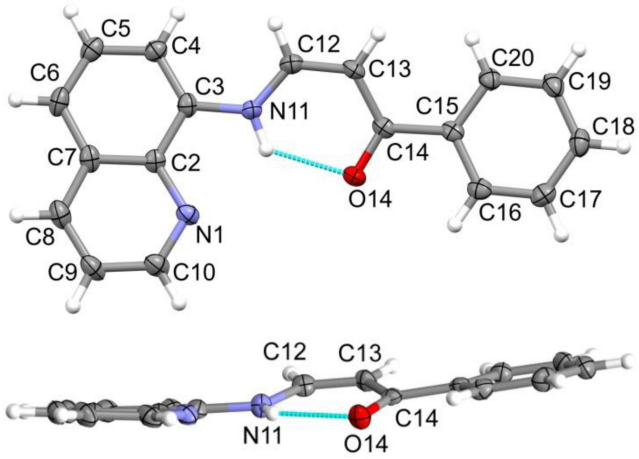

Figure 4. Two projection of the molecule in the single crystal of 1-phenyl-3-(quinolin-8-ylamino)prop-2-en-1-one with a numbering scheme. The displacements of the ellipsoids are drawn with a probability level of 50%. The hydrogen atoms are represented as fixed-size spheres. H-bonds are shown by blue dashed lines.

an angle of 178.1(1)° between themselves. Thus, complete conjugation of aromatic fragments in the molecule is not observed. Note that intramolecular hydrogen bonding N11–H11…N1 (d(N11–H11) 0.91(3) Å, d(H11… N(1) 2.26(3) Å, d(N11… N(1) 2.685(3) Å, ∠(N11–H11… N(1) 108(2)°) is observed, although its parameters exceed the formal criteria for the formation of hydrogen bonds, for example, accepted in the PLATON program. The supramolecular structure of the single crystal is shown in Supporting Information.

Analysis of NMR spectra

The assignment of ^{1}H and ^{13}C NMR signals to hydrogen and carbon atoms of the molecules of 1-phenyl-3-(quinolin-8-ylamino)prop-2-en-1-one in the solutions was performed by the ratios between integrated intensities of the signals and 2D NMR spectra (^{1}H–^{1}H COSY, ^{1}H–^{13}C HSQC and HMBC spectra are shown in Supporting Information).

The listed below ^{1}H and ^{13}C NMR resonances were assigned to the hydrogen and carbon atoms of the molecule in accordance with the numbering scheme shown in Figure 4.

^{1}H NMR (CCl_4, 400 MHz): δ = 13.09 (d, J = 12.7 Hz, 1H, H11), 8.98 (dd, J = 1.1 Hz and 4.0 Hz, 1H, H10), 8.02 (dd, J = 1.1 Hz and 8.1 Hz, 1H, H8), 7.91 (dd, J = 7.9 Hz and 1.9 Hz, 2H, H16 and H20), 7.56 (dd, J = 8.1 Hz and 12.7 Hz, 1H, H12), 7.27–7.42 (m, 7H, H4, H5, H6, H9, H17, H18 and H19), 6.04 (d, J = 8.1 Hz, 1H, H13) ppm.

^{13}C NMR (CCl_4, 100 MHz): δ = 189.5 (C14), 149.1 (C10), 141.2 (C12), 140.0 (C15), 139.4 (C2), 138.7 (C3), 135.7 (C8), 131.4 (C18), 129.2 (C7), 128.5 (C17 and C19), 128.1 (C16 and C20), 127.0 (C5), 122.2 (C9), 120.7 (C6), 109.1 (C4), 95.8 (C13) ppm.

^{1}H NMR ($(CD_3)_2CO$, 400 MHz): δ = 13.25 (d, J = 11.2 Hz, 1H, H11), 9.00 (dd, J = 4.1 Hz and 1.7 Hz, 1H, H10), 8.36 (dd, J = 8.3 Hz and 1.7 Hz, 1H, H8), 8.01–8.08 (m, 3H, H12, H16 and H20), 7.73 (dd, J = 6.6 Hz and 2.2 Hz, 1H, H4), 7.49–7.64 (m, 6H, H5, H6, H9, H17, H18 and H19), 6.31 (d, J = 8.1 Hz, 1H, H13) ppm.

^{13}C NMR ($(CD_3)_2CO$, 100 MHz): δ = 190.9 (C14), 150.1 (C10), 143.4 (C12), 140.4 (C15), 139.3 (C2), 138.3 (C3), 137.0 (C8), 132.4 (C18), 129.8 (C7), 129.3 (C17 and C19), 128.3 (C16 and C20), 127.9 (C5), 123.2 (C9), 122.1 (C6), 110.6 (C4), 95.8 (C13) ppm.

^{1}H NMR ($(CD_3)_2SO$, 400 MHz): δ = 13.14 (d, J = 13.0 Hz, 1H, H11), 9.02 (dd, J = 4.2 Hz and 1.7 Hz, 1H, H10), 8.40 (dd, J = 8.3 Hz and 1.6 Hz, 1H, H8), 8.15 (dd, J = 13.0 Hz and 8.3 Hz, 1H, H12), 8.03 (m, 2H, H16 and H20), 7.83 (dd, J = 7.5 Hz and 1.3 Hz, 1H, H4), 7.50–7.67 (m, 6H, H5, H6, H9, H17, H18 and H19), 6.30 (d, J = 8.0 Hz, 1H, H13) ppm.

^{13}C NMR ($(CD_3)_2SO$, 100 MHz): δ = 189.5 (C14), 149.4 (C10), 143.4 (C12), 138.8 (C15), 137.5 (C2), 136.5 (C3), 136.4 (C8), 131.8 (C18), 128.6 (C17 and C19), 128.4 (C7), 127.3 (C16 and C20), 127.1 (C5), 122.5 (C9), 121.4 (C6), 110.3 (C4), 94.8 (C13) ppm.

Figures 5 and 6 show a comparison of the ^{1}H and ^{13}C NMR spectra of the substance in the above-mentioned solvents. The strong difference in the NMR spectra of these solutions can be explained by the different polarity of the solvent molecules,[42–46] since the electric dipole moments of the solvent molecules affect the distribution of electron density throughout the molecule of the studied substance and, consequently, on the degree of shielding of nuclei by their electron shells. This substance has already been studied by NMR in deuterated chloroform[6] (it should be noted that the authors of that paper made a misprint when interpreting the ^{1}H NMR spectrum of this compound – the proton with δ = 13.34 ppm was designated by

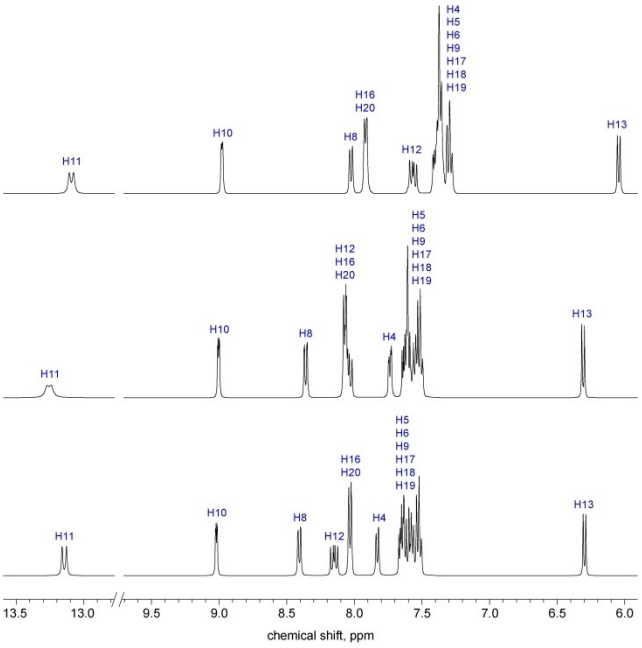

Figure 5. ^{1}H NMR spectra of 1-phenyl-3-(quinolin-8-ylamino)prop-2-en-1-one in solutions of carbon tetrachloride (top), deuterated acetone (middle) and dimethyl sulfoxide (bottom).

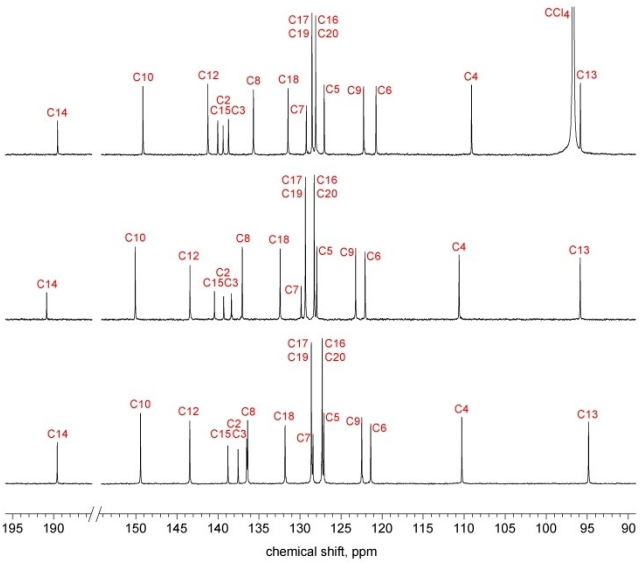

Figure 6. ^{13}C NMR spectra of 1-phenyl-3-(quinolin-8-ylamino)prop-2-en-1-one in solutions of carbon tetrachloride (top), deuterated acetone (middle) and dimethyl sulfoxide (bottom).

them as H_{3a}, but it would be correct to denote that as H_{8b}). Despite the fact that the ^{1}H NMR spectra of the substance in chloroform and carbon tetrachloride differ from each other, many of the splitting constants of the ^{1}H NMR signals are almost the same (for example, 12.9 Hz vs. 12.7 Hz for the proton H11, 8.0 Hz vs. 8.1 Hz for the proton H13, 4.2 Hz vs. 4.0 Hz for the proton H10, 8.0 Hz vs. 8.1 Hz for the proton H8, 8.0 Hz vs. 7.9 Hz for the protons H16 and H20). Since the splitting constants of ^{1}H NMR signals depend on many factors characterizing the structure of the molecule (such as the lengths of chemical bonds, dihedral angles between bonds, etc.), the coincidence of these constants indicates the similarity of the structure of the molecule of the substance in solutions of chloroform and carbon tetrachloride.

Chemical shifts of the signals, the values of their splitting, as well as cross-peaks in 2D NMR spectra allows us to find out exactly what isomers of 1-phenyl-3-(quinolin-8-ylamino)prop-2-en-1-one are present in the studied solutions. If the ketoimine isomer (**A**) would be present in any of the studied solutions, then the H11 hydrogen atom would be absent in this solution, and the C13 carbon would be bonded not to one hydrogen atom, but to two hydrogen atoms (see Figure 1). This would lead to the fact that the ^{1}H NMR signal with a chemical shift $\delta >$ 13 ppm would disappear, and the signal of H13 protons would be observed not in the range of 6.0–6.3 ppm, but in the range of 3.5–4.5 ppm which is typical of CH_2 groups of the ketoimine isomer of the molecules having a phenyl and pyridine rings as well as the characteristic pentad of atoms O–C–C–C–N (see, for example, ^{1}H chemical shifts of CH_2 groups of compound K in[22]). However, only signals of the solvents are observed in the chemical shift range of 0–6 ppm in the ^{1}H NMR spectra of 1-phenyl-3-(quinolin-8-ylamino)prop-2-en-1-one in the given solutions (this region of the spectra is shown in Supporting Information).

Because in the *cis*- and *trans*-forms of the enaminoketone isomer (**B**) the hydrogen atom H11 is bonded to the nitrogen atom N11, the closest hydrogen atom to H11 is the H12 atom. In the enolimine isomer (**C**), the hydrogen atom H11 is bonded to the oxygen atom O14, so the closest hydrogen atom to H11 is the H13 atom. As is well known, the dipole-dipole interaction of nuclear spins in solutions is averaged to zero, therefore only the scalar J-coupling leads to the splitting of the signals in NMR spectra of solutions. The nuclear spins of the hydrogen atoms H11 and H12 in the *cis*- and *trans*-forms of the enaminoketone isomer (**B**) will interact with each other through three chemical bonds H11–N11–C12–H12, and in the enolimine isomer (**C**) the nuclear spins H11 and H13 will interact with each other through four chemical bonds H11–O14–C14–C13–H13. The scalar J-coupling decreases sharply with increasing number of chemical bonds between interacting spins. The scalar J-coupling constants of protons interacting with each other through three chemical bonds ^{3}J are in the range of 0–24 Hz and through four chemical bonds ^{4}J are in the range of 0–4 Hz.[47] There are extremely rare exceptions when ^{4}J is equal to 18 Hz, but this is possible only in very strained molecules, such as bicyclo[1.1.1]-pentane,[48] where several routes are available for coupling between the protons. But in the enolimine isomer (**C**) there is only one such route for the nuclear spins H11 and H13, therefore their coupling constant ^{4}J should be no more than 4 Hz. However, in the all three solutions of 1-phenyl-3-(quinolin-8-ylamino)prop-2-en-1-one the splitting constants of the H11 proton signal are equal to 11–13 Hz, consequently in these solutions the molecules of the substance are the *cis*- or the *trans*-form of the enaminoketone isomer (**B**) (see Figure 1).

The *cis*- and *trans*-forms of the enaminoketone isomer (**B**) have the same chemical structure, but different spatial con-

struction. The transformation from one form to another occurs as a result of rotation of one part of the molecule relative to another part around the double bond C12–C13. As a consequence, in the *cis*- and *trans*-forms the scalar J-coupling constants between the H12 and H13 protons will differ from each other, because according to the Karplus equation the coupling constant ^{3}J depends on the dihedral angle between the H12–C12–C13 and C12–C13–H13 planes. As a rule, the scalar J-coupling constant in the *trans*-conformation is greater than in the *cis*-conformation.[47, 26] Consequently, if we could induce *cis-trans*-isomerization of 1-phenyl-3-(quinolin-8-ylamino)prop-2-en-1-one molecules, then on the base of the change in the coupling constant ^{3}J we could determine which form of the enaminoketone isomer (**B**) (*cis*- or *trans*–) is present in the initial solutions.

In many compounds containing a C=C or N=N double bond, the *cis-trans*-isomerization is induced by UV irradiation.[49–53,15] However, irradiation of the all three solutions of 1-phenyl-3-(quinolin-8-ylamino)prop-2-en-1-one with UV light does not lead to the *cis-trans*-isomerization, but it results in the formation of a brown precipitate. This precipitate is poorly soluble in many organic solvents, however is quite soluble in chloroform. The chemical shifts and relative intensities of the signals in the region of 6–11 ppm in the ^{1}H NMR spectrum of the brown precipitate (recorded in a solution of deuterated chloroform) indicate that most likely it consists of heterocyclic compounds (this spectrum is shown in Supporting Information).

A strong change in the polarity of the solvent from nonpolar carbon tetrachloride to highly polar dimethyl sulfoxide also does not lead to *cis-trans*-isomerization, since the value of the splitting of the H13 proton (equal to the scalar J-coupling constant of the H12 and H13 protons) in the studied solutions is the same and equal to 8.05 ± 0.05 Hz. It is obvious that this method is unpromising, therefore in order to distinguish between *cis*- and *trans*-isomers, 2D NOESY NMR spectroscopy was used.

NOESY spectroscopy is based on the nuclear Overhauser effect and allows us to identify spins undergoing cross-relaxation. The intensity of cross-peaks in NOESY spectra depends on the distance r between cross-relaxing spins as $1/r^6$, therefore, the closer the spins are located to each other in space, the more intense cross-peaks corresponding to these spins will be observed. For the enaminoketone isomer (**B**) the distance both between the spins H13–H12 and between the spins H13–H11 greatly depends on the fact that in *cis*- or in *trans*-form the molecule is. In the *cis*-form the distance between the spins H13–H12 is about 2.4Å and the distance between the spins H13–H11 is about 3.7Å, so that the cross-peak H13–H12 should be much more intense than the cross-peak H13–H11. In the *trans*-form the distance between the spins H13–H12 is about 3.1Å and the distance between the spins H13–H11 is about 2.5Å, so that the cross-peak H13–H11 should be much more intense than the cross-peak H13–H12. In the NOESY spectra of 1-phenyl-3-(quinolin-8-ylamino)prop-2-en-1-one in the all three solutions an intense cross-peak H13–H12 is visible, and the cross-peak H13–H11 is either very weak or not visible at all (they are shown in Supporting Information). Consequently, the *cis*-form of the enaminoketone isomer (**B**) is present in the studied solutions of the substance.

Exposing the solutions of 1-phenyl-3-(quinolin-8-ylamino)prop-2-en-1-one in acetone and DMSO to light at room temperature for several months leads to the formation in them of a small amount of the *trans*-isomer (~7 %). Low-intensity ^{1}H NMR signals corresponding to the most of the protons of the *trans*-isomer of the substance overlap with the intense signals of the *cis*-isomer and are not visible among them. However, some NMR signals of the *trans*-isomer are located separately from the signals of the *cis*-isomer. In order to identify these signals, we used the fact that *cis-trans*-isomerization leads to a change only in the scalar J-coupling constants of the H12 and H13 protons (see Figure 4), which interacting with each other through a double C=C bond, whereas the scalar J-coupling constants of the rest of protons should remain almost unchanged. In the $(CD_3)_2CO$ solution the following signals of the *trans*-isomer were observed: 9.77 (d, J = 12.9 Hz, 1H, H11), 8.84 (dd, J = 4.2 Hz and 1.7 Hz, 1H, H10), 8.49 (t, J = 12.7 Hz and 12.9 Hz, 1H, H12), 7.10 (d, J = 12.7 Hz, 1H, H13) ppm, while in the $(CD_3)_2SO$ solution the observed signals were: 10.35 (d, J = 13.1 Hz, 1H, H11), 8.93 (dd, J = 4.2 Hz and 1.7 Hz, 1H, H10), 7.94 (dd, J = 8.3 Hz and 1.6 Hz, 1H, H8), 7.11 (d, J = 12.6 Hz, 1H, H13) ppm.

Molecular geometries and energies from DFT calculations

The calculated ground state energies of isomers and tautomers of the molecule are presented in Table 2. The *cis*-isomer is energetically more favorable, but the total ground state energy of the *cis*-isomer is only 0.093 eV more favorable than the energy of the *trans*-isomer.

For all isomers and tautomers, absorption spectra were calculated by the ESD method (Excited States Dynamic, taking into account vibrational modes).[54] Within the framework of the ESD method, a search for the optimal geometry of the ground state (see Figure 7) and the first excited state was carried out with the calculation of Hessian for each state separately (AH method). Knowing the square of the length of the displacement vector of the geometry of the ground state relative to the geometry of the first excited state is very important for this technique: if the square of the length of the displacement vector is 8 or more, then this technique may not work. The ORCA software package also has several other methods for

Table 2. Ground state energies of isomers and tautomers of the molecule and the energy difference relative to the minimum energy value calculated by the DFT method.

Conformation	E, eV	ΔE, eV
B	−23916.820	0
trans-	−23916.727	0.093
C	−23916.400	0.42
A	−23916.167	0.65

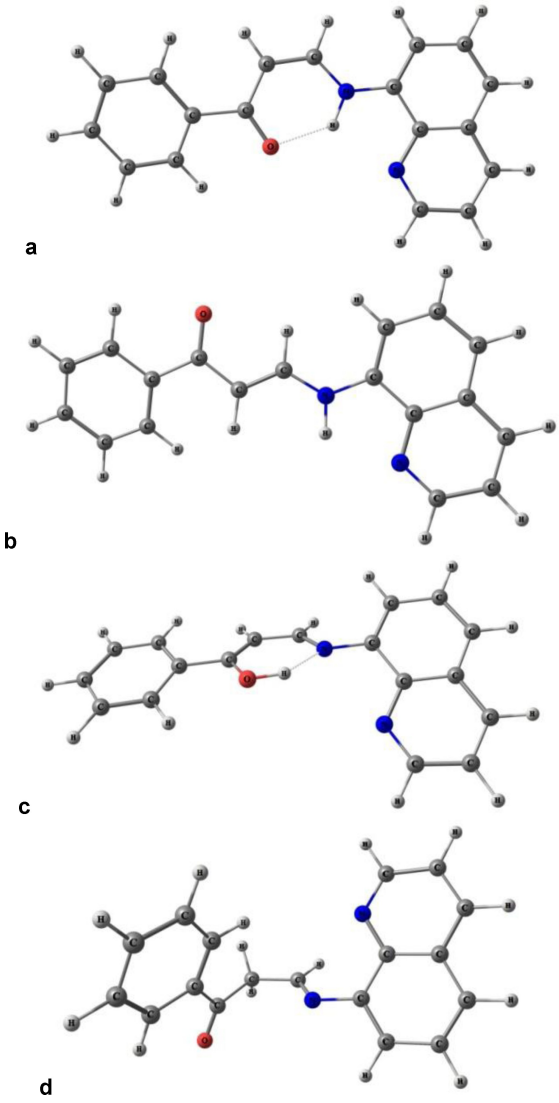

Figure 7. Optimized geometries of isomers and tautomers of the molecule of 1-phenyl-3-(quinolin-8-ylamino)prop-2-en-1-one: (**a**) cis-isomer, (**b**) trans-isomer, (**c**) enolomine tautomer, (**d**) ketoimine tautomer. Here red balls are oxygen atoms, blue balls are nitrogen atoms, dark gray balls are carbon atoms, light gray balls are hydrogen atoms.

finding the potential energy surface (PES) for the excited state: AHAS, VG and VH, which differ in different ways of calculating the matrix of second derivatives of the excited state (ES Hessian). Thus, in the AHAS (Adiabatic Hessian After Step) method, ES Hessian is calculated for the geometry, which is obtained as a result of a geometry update step along the PES, depending on the gradient of the excited state and the Hessian of the ground state. The AH method was used in order to calculate the absorption spectra of the *cis*-isomer, the *trans*-isomer and ketoimine tautomer, but for the enolimine tautomer the AHAS method was used due to the large square of the length of the displacement vector. The calculated absorption spectra are presented in Figure 8.

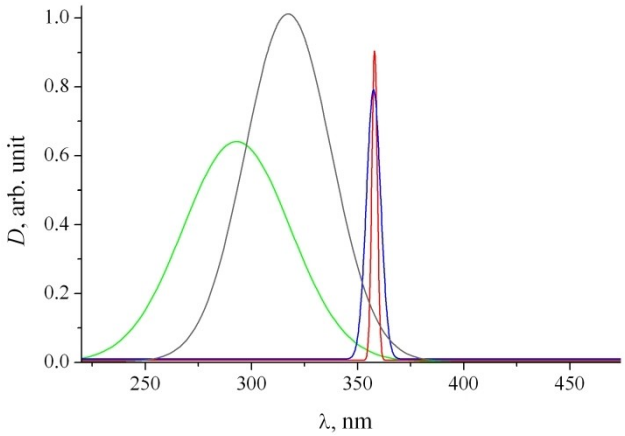

Figure 8. UV absorption spectra corresponding to various conformations of 1-phenyl-3-(quinolin-8-ylamino)prop-2-en-1-one: the cis-isomer (blue), the trans-isomer (red), the enolimine tautomer (grey) and the ketoimine tautomer (green).

Analysis of Uv-vis spectra

The electronic spectra of 1-phenyl-3-(quinolin-8-ylamino)prop-2-en-1-one were recorded in different solvents and under the influence of temperature and light irradiation with $\lambda = 365$ nm. The bathochromic shift of all absorption bands indicates the delocalization of electrons in the molecule of the substance.

The electronic spectra of the solutions of the studied substance demonstrate low-intensity broad excitation band of π-electrons of the aromatic system, which is in the range $\lambda_{max} =$ 325–329 nm and weakly dependent on the polarity of the solvent (see Figure 9). This band is partially overlapped by the intense band of the π–π^* transition. In acetone, the absorption band of the benzene ring is not visible at all, since it is hidden by the solvent band. Changing the solvent polarity had weak effect on this band that confirms the local nature of its electronic transition. This band indicates that the benzene ring deviates from the plane of the central part of the molecule,

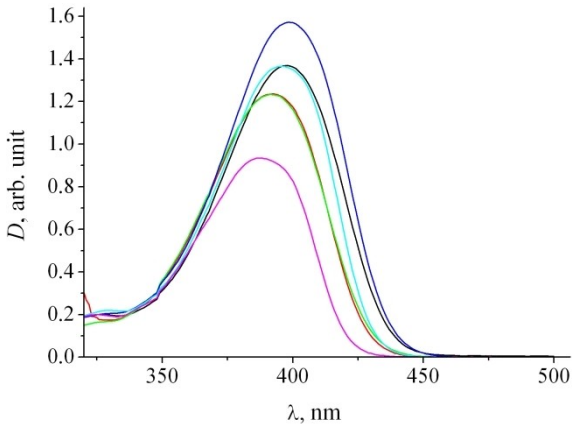

Figure 9. UV-Vis spectrum of 1-phenyl-3-(quinolin-8-ylamino)prop-2-en-1-one recorded at a concentration of 4.4×10^{-5} mol/L in different solvents: chloroform (black), acetone (red), acetonitrile (green), carbon tetrachloride (blue), hexane (purple).

leading to incomplete conjugation of aromatic fragments in the molecule both in all solutions and in the solid state. The same conclusion follows from the results of both the DFT calculations and the X-ray crystallography of the grown single crystal of 1-phenyl-3-(quinolin-8-ylamino)prop-2-en-1-one.

Intense absorption bands in the range of 388–399 nm are attributed to the π–π* transition (exact λ values corresponding to the maxima of the π-π* absorption bands at 25°C, as well as the extinction coefficients of 1-phenyl-3-(quinolin-8-ylamino)-prop-2-en-1-one in various solvents are listed in Table 3). Structural transformations of molecules are most easily observed just on the basis of changes in this band, since the π–π* transition is sensitive to the polarity of the solvent and the effect of conjugation of double bonds in molecules. The increase the polarity of the solvent usually results in a bathochromic shift of the absorption bands indicating that the molecule in the excited state is more polar than in the ground state.[55] Absorption bands of the studied substance in CCl_4 and $CHCl_3$ solutions are bathochromically shifted relative to the bands observed in solutions of the substance in more polar acetone and acetonitrile.

Table 3. UV absorption data of 1-phenyl-3-(quinolin-8-ylamino)prop-2-en-1-one in different solvents at a concentration of 4.4×10^{-5} mol/L.

Solvent	$\lambda_{\pi-\pi^*}$, nm at 25°C	ε_{max}, $dm^3\ cm^{-1}\ mol^{-1}$
hexane	388	21239
carbon tetrachloride	395	31018
chloroform	397	31107
Acetone	392	28082
Acetonitrile	391	28016
dimethyl sulfoxide	399	35711

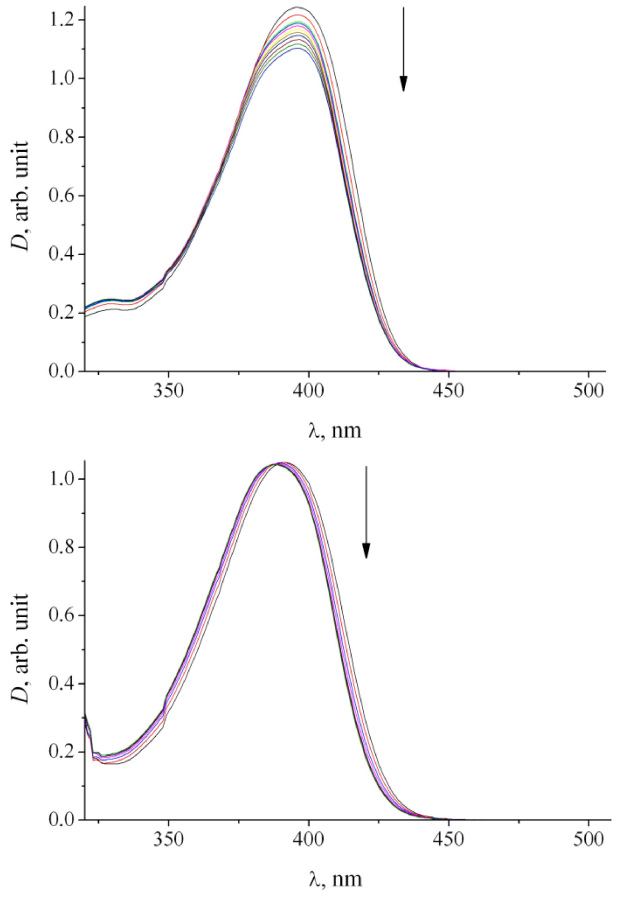

Figure 10. UV-vis spectra of 1-phenyl-3-(quinolin-8-ylamino)prop-2-en-1-one during UV irradiation within 2 min in an carbon tetrachloride solution (top) at a concentration of 3.4×10^{-5} mol/L and in an acetone (bottom) solution at a concentration of 2.5×10^{-5} mol/L.

The solutions were irradiated with UV light at 365 nm (see Figure 10). The hypochromic effect observed during irradiation correlates with the polarity of the solvents: the UV irradiation of the solutions during 2 minutes causes a decrease in the intensity of the bands the π–π* transition by 0.0359, 0.0083 and 0.0008 for CCl_4, acetone and DMSO, respectively. Such correlation indicates an increase in the strength of intermolecular interactions between the solute and the solvent in this series. Thus, we can conclude that during the irradiation of solutions at least a weakening and partial breaking of the intermolecular bonds of the substance with the solvent occurs in them.[56]

Conclusions

In the present work the synthesis of 1-phenyl-3-(quinolin-8-ylamino)prop-2-en-1-one is described and the possible reaction mechanism is proposed. This compound exists in the solid state in the β-enaminoketone form of the cis-isomer and is stabilized by intramolecular hydrogen bonding. In the crystal the geometry of the molecule is close to flat, but due to small deviations of its fragments from the plane, a complete electronic conjugation of aromatic rings in the molecule is not observed. In the dissolved state, regardless of the polarity of the solvent, the molecules are also in a stable enaminoketone form of the cis-isomer, which is stabilized owing to forming the pseudo-aromatic ring. Despite the fact that the total energies of the ground state of the cis-isomer and trans-isomer are very close (−23916.820 and −23916.727 eV from the results of the DFT calculations), a small amount (~7%) of the trans-isomer is formed only when the substance is kept in acetone and DMSO for a long time (more than two month) in daylight.

Supporting Information Summary

Supporting Information contains the ^{1}H NMR spectrum of the brown precipitate dissolved in deuterated chloroform and formed by 365 nm UV-light irradiation of 1-phenyl-3-(quinolin-8-ylamino)prop-2-en-1-one molecules in carbon tetrachloride; 2D NMR COSY, NOESY, HSQC and HMBC spectra of the substance in carbon tetrachloride, deuterated acetone and deuterated dimethyl sulfoxide; 3D-supramolecular structure formed in 1-phenyl-3-(quinolin-8-ylamino)prop-2-en-1-one single crystal and also a UV-vis spectrum of the substance in dimethyl sulfoxide at 70°C and at room temperature.

Crystallographic data

Crystallographic data (excluding structure factors) for the investigated structure has been deposited in the Cambridge Crystallographic Data Centre as supplementary publication number CCDC 2279360. Copies of the data can be obtained free of charge upon application to CCDC, 12 Union Road, Cambridge CB2 1EZ, UK (fax: 44(0)1223 336033; e-mail: deposit@ccdc.cam.ac.uk).

Acknowledgements

This work was performed by the financial support from the government assignment for Federal Research Center of Kazan Scientific Center of Russian Academy of Sciences.

Conflict of Interests

The authors declare no conflict of interest.

Data Availability Statement

Crystallographic data (excluding structure factors) for the investigated structure has been deposited by us in the Cambridge Crystallographic Data Centre as supplementary publication number CCDC 2279360. Copies of the data can be obtained free of charge upon application to the CCDC (12 Union Road, Cambridge CB2 1EZ UK. Fax: (internat.) +44-1223/336-033; E-mail: deposit@ccdc.cam.ac.uk).

Keywords: β-Enaminone · DFT · NMR · UV-Vis · X-ray

[1] J. Huang, F. Yu, *Synthesis.* **2021**, *53*, 587.
[2] A. Z. Elassar, A. A. El-Khair, *Tetrahedron.* **2003**, *59*, 8463.
[3] Y. F. Freimanis, Chemistry of enaminoketones, enaminoimines, and enaminothiones [in Russian], Zinatne, Riga, **1974**.
[4] D. V. Dar'in, P. S. Lobanov, *Russ. Chem. Rev.* **2015**, *84*, 601.
[5] I. J. Amaye, R. D. Haywood, E. M. Mandzo, J. J. Wirick, P. L. Jackson-Ayotunde, *Tetrahedron.* **2021**, *83*, 131984.
[6] S. Khanikar, S. Kaping, P. Helissey, P. Joshi, S. H. Shaham, S. Mishra, M. Srivastava, R. Tripathi, J. N. Vishwakarma, *Monatsh. Chem.* **2021**, *152*, 665.
[7] H. A. El-Ghamry, K. Yamauchi, K. Sakai, T. A. Farghaly, *Inorg. Chim. Acta.* **2021**, *516*, 120117.
[8] Y. C. Shi, C. X. Sui, H. B. Song, P. M. Jian, *J. Coord. Chem.* **2005**, *58*, 363.
[9] T. V. Kovaleva, A. I. Uraev, K. A. Lyssenko, V. G. Vlasenko, A. S. Burlov, G. S. Borodkin, D. A. Garnovskii, *Rus. J. Coord. Chem.* **2022**, *48*, 210.
[10] H. Kurz, K. Schötz, I. Papadopoulos, F. W. Heinemann, H. Maid, D. M. Guldi, A. Köhler, G. Hörner, B. Weber, *J. Am. Chem. Soc.* **2021**, *143*, 3466.
[11] K. Dankhoff, B. Weber, *Dalton Trans.* **2019**, *48*, 15376.
[12] M. G. Siegel, J. D. Winkler, Photochemistry of enamines and enaminones. Chapter 11 of the book "The Chemistry of Enamines", edited by Zvi Rappoport. John Wiley & Sons, **1994**.
[13] C. Dugave, L. Demange, *Chem. Rev.* **2003**, *103*, 2475.
[14] J. Sitkowski, W. Bocian, A. Szterk, *J. Mol. Struct.* **2018**, *1171*, 449.
[15] A. F. Shaidullina, A. R. Sharipova, M. Yu Volkov, L. I. Savostina, L. G. Gafiyatullin, O. A. Turanova, A. N. Turanov, *Photochem. Photobiol.* **2023**, *99*, 1378.
[16] H. Li, H. Shu, X. Wang, X. Wu, H. Tian, H. Tong, L. Wang, *Org. Mater.* **2020**, *02*, 33.
[17] J. V. Greenhill, H. Loghmani-Khouzani, D. J. Maitland, *J. Chem. Soc.-Perkin Trans.* **1991**, *1*, 2831.
[18] C. A. Grob, H. J. Wilkens, *Helv. Chim. Acta.* **1967**, *50*, 725.
[19] A. I. Kol'tsov, G. M. Kheifets, *Russ. Chem. Rev.* **1972**, *41*, 452.
[20] R. Dobosz, J. Mucko, R. Gawinecki, *Energies.* **2020**, *13*. 183.
[21] A. Rybarczyk-Pirek, S. J. Grabowski, M. Malecka, J. Nawrot-Modranka, *J. Phys. Chem. A.* **2003**, *106*, 11956.
[22] E. Kolehmainen, B. Osmialowski, T. M. Krygowski, R. Kauppinen, M. Nissinen, R. Gawinecki, *J. Chem. Soc.-Perkin Trans.* **2000**, *2*, 1259.
[23] R. Yoshii, A. Nagai, K. Tanaka, Y. Chujo, *Macromol. Rapid Commun.* **2014**, *35*, 1315.
[24] G. R. Fulmer, A. J. M. Miller, N. H. Sherden, H. E. Gottlieb, A. Nudelman, B. M. Stoltz, J. E. Bercaw, K. I. Goldberg, *Organometallics.* **2010**, *29*, 2176.
[25] Wiley SpectraBase. SpectraBase Compound ID Jk7oLgP89yO. Available online: https://spectrabase.com/spectrum/9th8qziEnuX.
[26] Bruker Almanac 2011. Tables and other useful information. Chemical tables. Properties of selected nondeuterated solvents. Bruker BioSpin GmbH (Germany), 2011, https://lsa.umich.edu/content/dam/chem-assets/chem-docs/BrukerAlmanac2011.pdf.
[27] A. A. Shaw, C. Salaun, J. F. Dauphin, B. Ancian, *J. Magn. Reson. Ser. A* **1996**, *120*, 110.
[28] B. Ancian, I. Bourgeois, J. F. Dauphin, A. A. Shaw, *J. Magn. Reson.* **1997**, *125*, 348.
[29] J. Jeener, B. H. Meier, P. Bachmann, R. R. Ernst, *J. Chem. Phys.* **1979**, *71*, 4546.
[30] J. Schleucher, M. Schwendinger, M. Sattler, P. Schmidt, O. Schedletzky, S. J. Glaser, O. W. Sorensen, C. Griesinger, *J. Biomol. NMR.* **1994**, *4*, 301.
[31] A. G. Palmer, J. Cavanagh, P. E. Wright, M. Rance, *J. Magn. Reson.* **1991**, *93*, 151.
[32] A. Bax, M. F. Summers, *J. Am. Chem. Soc.* **1986**, *108*, 2093.
[33] G. Sheldrick, SADABS, Program for empirical X-ray absorption correction, Bruker-Nonius, **2004**.
[34] G. Sheldrick, SHELXTL v.6.12, Structure Determination Software Suite, Bruker AXS, Madison, Wisconsin, USA, **2000**.
[35] APEX2 (Version 2.1), SAINTPlus, Data Reduction and Correction Program (Version 7.31 A), BrukerAXS Inc., Madison, Wisconsin, USA, **2006**.
[36] L. J. Farrugia, *J. Appl. Crystallogr.* **1999**, *32*, 837.
[37] A. L. Spek, *J. Appl. Crystallogr.* **2003**, *36*, 7.
[38] I. J. Bruno, J. C. Cole, P. R. Edgington, M. Kessler, C. F. Macrae, P. McCabe, J. Pearson, R. Taylor, *Acta Crystallogr. Sect. B* **2002**, *58*, 389.
[39] F. Neese, *WIREs Comput. Mol. Sci.* **2012**, *2*, 73.
[40] T. Yanai, D. P. Tew, N. C. Handy, *Chem. Phys. Lett.* **2004**, *393*, 51.
[41] F. Weigend, *Phys. Chem. Chem. Phys.* **2005**, *7*, 3297.
[42] M. A. Weinberger, R. M. Heggie, H. L. Holmes, *Can. J. Chem.* **1965**, *43*, 2585.
[43] P. Laszlo, *Prog. Nucl. Magn. Reson. Spectrosc.* **1967**, *3*, 231.
[44] J. Ronayne, D. H. Williams, *Annu. Rep. NMR Spectrosc.* **1969**, *2*, 83.
[45] J. Homer, *Appl. Spectrosc. Rev.* **1975**, *9*, 1.
[46] A. D. Buckingham, T. Schafer, W. G. Schneider, *J. Chem. Phys.* **1960**, *32*, 1227.
[47] H. Gunther, NMR spectroscopy. Basic principles, concepts and applications in chemistry. Third Edition. Wiley-VCH Verlag GmbH, Weinheim, Germany, **2013**.
[48] K. B. Wiberg, D. S. Connor, *J. Am. Chem. Soc.* **1966**, *88*, 4437.
[49] J. Konieczkowska, A. Wasiak, A. Sobolewska, S. Bartkiewicz, J. G. Malecki, E. Schab-Balcerzak, *J. Photochem. Photobiol. A.* **2023**, *444*, 114979.
[50] X. Sun, Z. Liu, Z. Wang, M. Huo, H. Y. Zhang, Y. Liu, *J. Org. Chem.* **2022**, *87*, 7658.
[51] C. P. Constantin, I. Sava, M. D. Damaceanu, *Macromolecules.* **2021**, *54*, 1517.
[52] O. A. Turanova, L. G. Gafiyatullin, O. I. Gnezdilov, A. N. Turanov, *Russ. J. Gen. Chem.* **2011**, *81*, 937.
[53] A. Mokdad, J. L. Belof, S. W. Yi, S. E. Shuler, M. L. McLaughlin, B. Space, R. W. Larsen, *J. Phys. Chem. A.* **2008**, *112*, 8310.
[54] B. de Souza, F. Neese, R. Izsak, *J. Chem. Phys.* **2018**, *148*, 034104.
[55] C. Reichardt, T. Welton, Solvents and solvent effects in organic chemistry. Weinheim WILEY-VCH, **2011**.
[56] V. Lazic, M. Jurkovic, T. Jednacak, T. Hrenar, P. J. Vukovic, P. Novak, *J. Mol. Struct.* **2015**, *1079*, 243.

Manuscript received: October 20, 2023